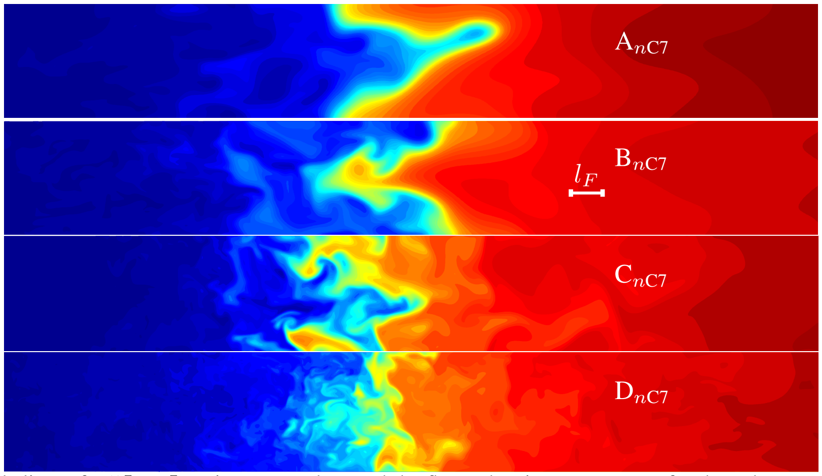

Fig. 1: Two-dimensional slices of a $5L \times L$ region centered around the flame showing temperature for the n-heptane non-unity Lewis number cases. The temperature ranges are [298, 2200] K for A and B and [800, 2400] K for C and D.

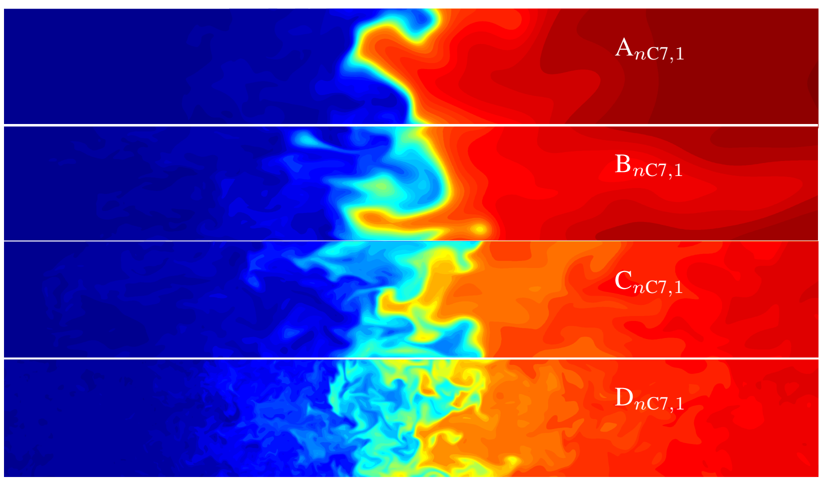

Fig. 2: Two-dimensional slices of a $5L \times L$ region centered around the flame showing temperature for the n-heptane unity Lewis number cases. The temperature ranges are [298, 2200] K for A and B and [800, 2400] K for C and D.

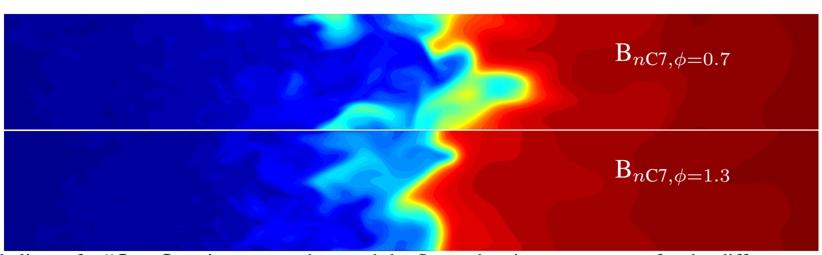

Fig. 3: Two-dimensional slices of a $5L \times L$ region centered around the flame showing temperature for the different equivalence ratios non-unity Lewis number cases. The temperature range is [298, 2200].

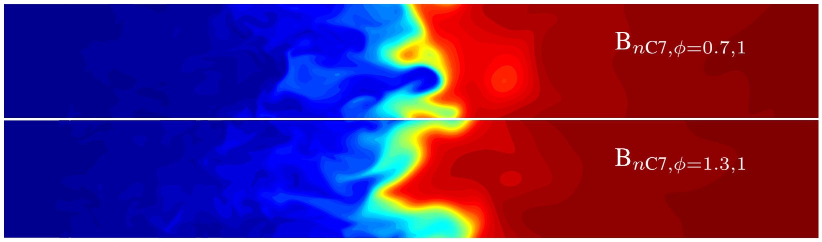

Fig. 4: Two-dimensional slices of a $5L \times L$ region centered around the flame showing temperature for the different equivalence ratios unity Lewis number cases. The temperature range is [298, 2200].

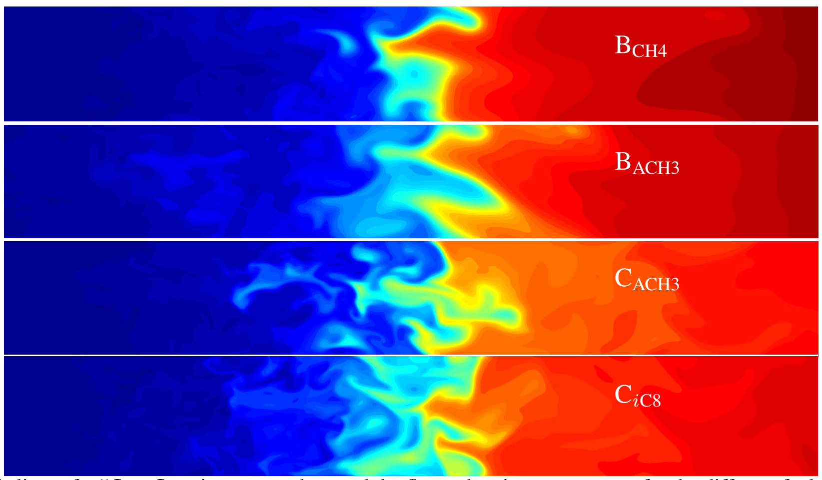

Fig. 5: Two-dimensional slices of a $5L \times L$ region centered around the flame showing temperature for the different fuels non-unity Lewis number cases. The temperature ranges are [298, 2200] K for A and B and [800, 2400] K for C and D.

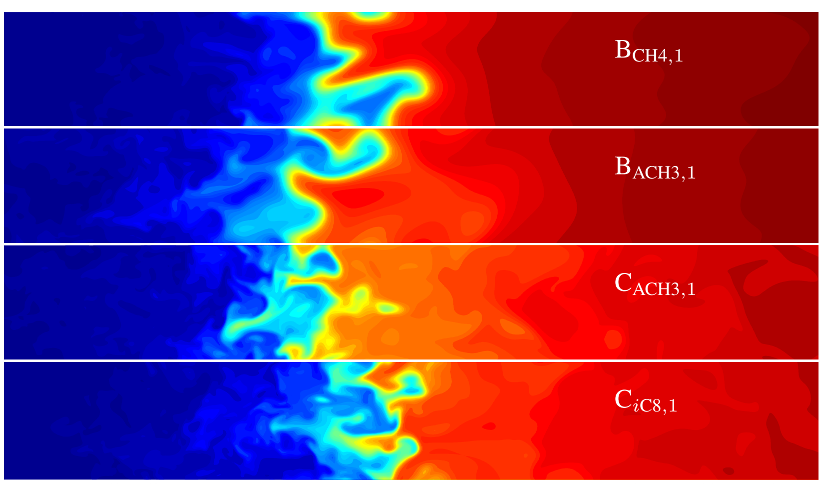

Fig. 6: Two-dimensional slices of a $5L \times L$ region centered around the flame showing temperature for the different fuels unity Lewis number cases. The temperature ranges are [298, 2200] K for A and B and [800, 2400] K for C and D.

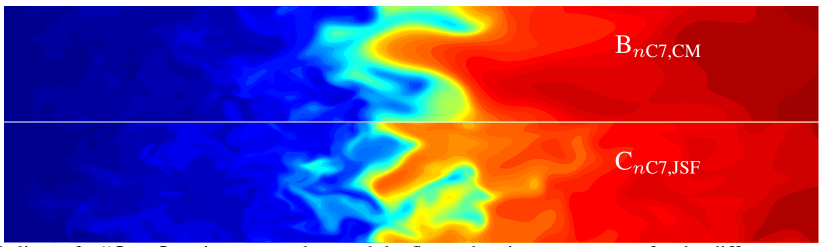

Fig. 7: Two-dimensional slices of a $5L \times L$ region centered around the flame showing temperature for the different mechanisms non-unity Lewis number cases. The temperature ranges are [298, 2200] K for A and B and [800, 2400] K for C and D.

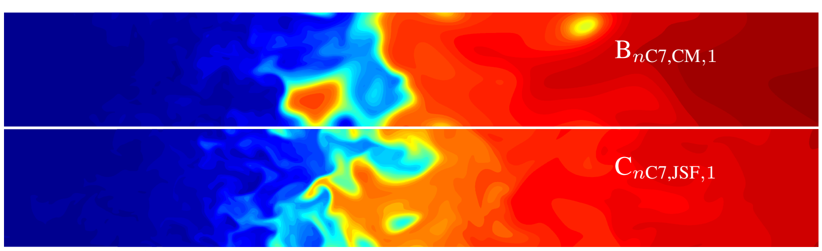

Fig. 8: Two-dimensional slices of a $5L \times L$ region centered around the flame showing temperature for the different mechanisms unity Lewis number cases. The temperature ranges are [298, 2200] K for A and B and [800, 2400] K for C and D.

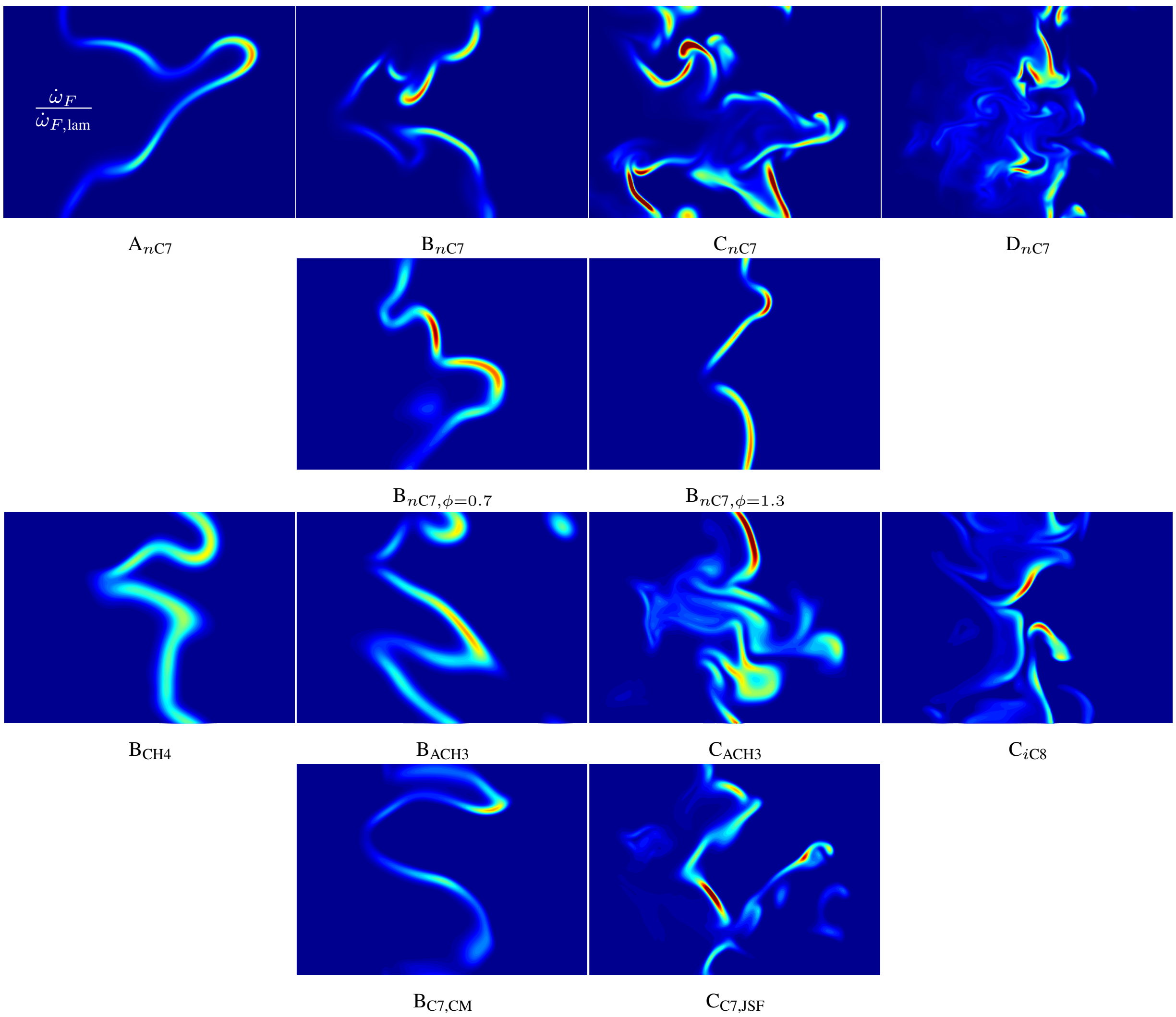

Fig. 9: Two-dimensional slices of a $1.3L \times L$ region centered around the flame showing fuel consumption rate (normalized by the peak value of the corresponding laminar flame). The fuel consumption rate range is satured at [0,2] in each case.

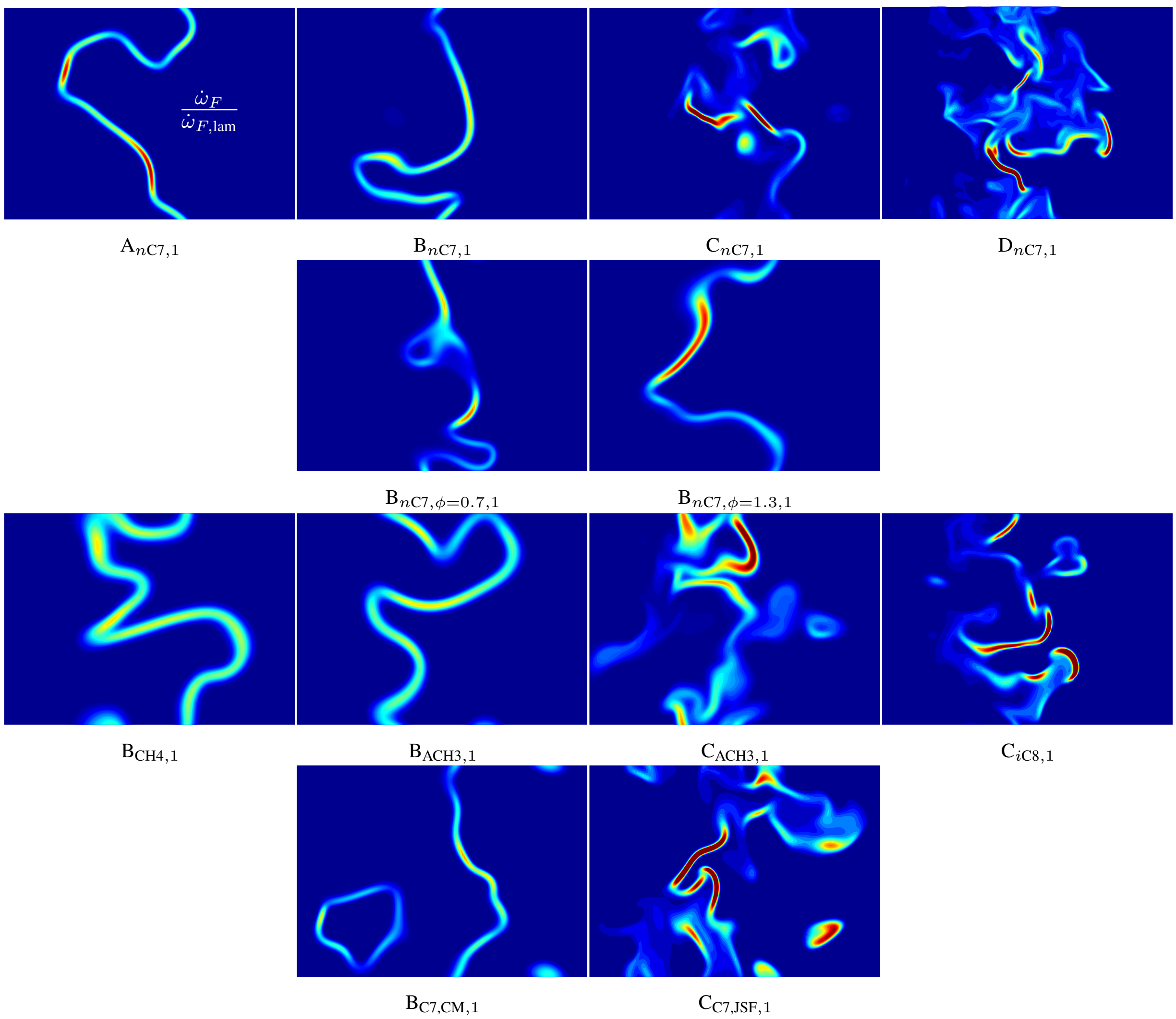

Fig. 10: Two-dimensional slices of a $1.3L \times L$ region centered around the flame showing the fuel consumption rate (normalized by the peak value of the corresponding laminar flame) for unity Lewis number cases. The fuel consumption rate range is satured at [0,2] in each case.

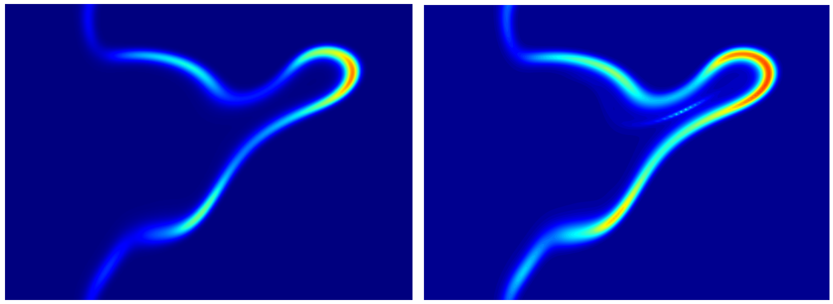

(a) $\dot{\omega}_F/\dot{\omega}_{F,\mathrm{lam}}$ (b) $(\dot{\omega}_F/|\nabla T|)/(\dot{\omega}_{F,\mathrm{lam}}/|\nabla T|_{\mathrm{lam}})$

Fig. 11: Instantaneous 2D slices of a $1.3L \times L$ region centered around the flame showing normalized fuel consumption rate and burning efficiency for case $\mathrm{A}_{n\mathrm{C7}}$.

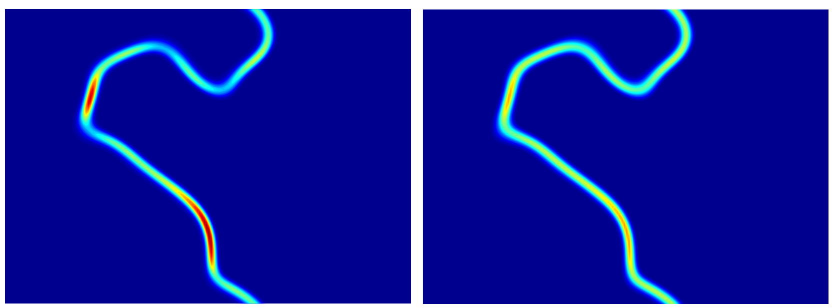

(a) $\dot{\omega}_F/\dot{\omega}_{F,\mathrm{lam}}$ (b) $(\dot{\omega}_F/|\nabla T|)/(\dot{\omega}_{F,\mathrm{lam}}/|\nabla T|_{\mathrm{lam}})$

Fig. 12: Instantaneous 2D slices of a $1.3L \times L$ region centered around the flame showing normalized fuel consumption rate and burning efficiency for case $\mathrm{A}_{n\mathrm{C7},1}$.

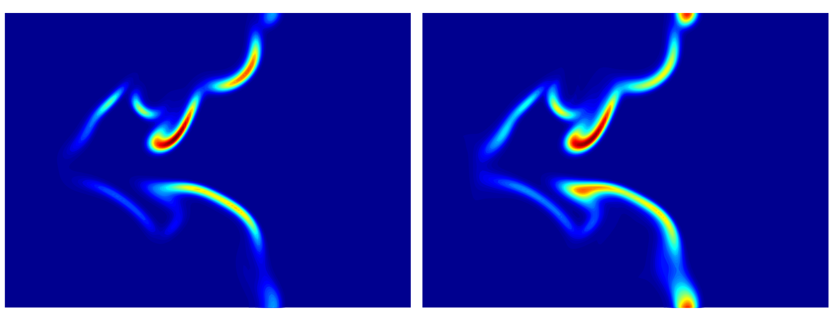

(a) $\dot{\omega}_F/\dot{\omega}_{F,\mathrm{lam}}$ (b) $(\dot{\omega}_F/|\nabla T|)/(\dot{\omega}_{F,\mathrm{lam}}/|\nabla T|_{\mathrm{lam}})$

Fig. 13: Instantaneous 2D slices of a $1.3L \times L$ region centered around the flame showing normalized fuel consumption rate and burning efficiency for case $\mathrm{B}_{n\mathrm{C7}}$.

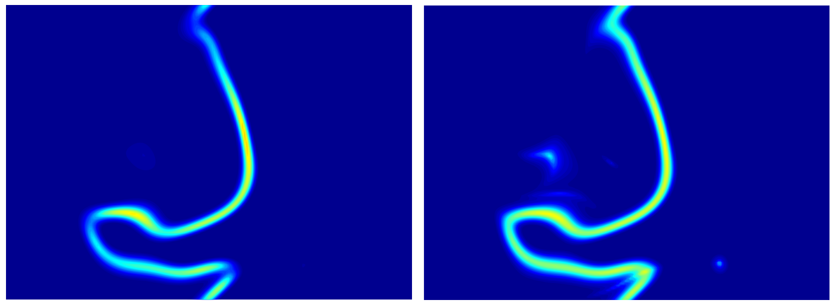

(a) $\dot{\omega}_F/\dot{\omega}_{F,\mathrm{lam}}$ (b) $(\dot{\omega}_F/|\nabla T|)/(\dot{\omega}_{F,\mathrm{lam}}/|\nabla T|_{\mathrm{lam}})$

Fig. 14: Instantaneous 2D slices of a $1.3L \times L$ region centered around the flame showing normalized fuel consumption rate and burning efficiency for case $\mathrm{B}_{n\mathrm{C}7,1}$.

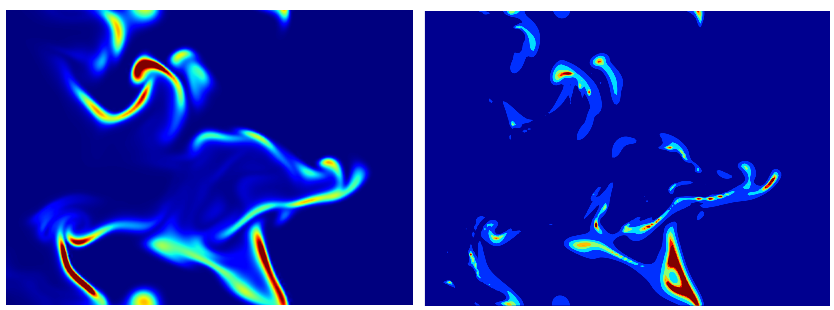

(a) $\dot{\omega}_F/\dot{\omega}_{F,\mathrm{lam}}$ (b) $(\dot{\omega}_F/|\nabla T|)/(\dot{\omega}_{F,\mathrm{lam}}/|\nabla T|_{\mathrm{lam}})$

Fig. 15: Instantaneous 2D slices of a $1.3L \times L$ region centered around the flame showing normalized fuel consumption rate and burning efficiency for case $\mathrm{C}_{n\mathrm{C}7}$.

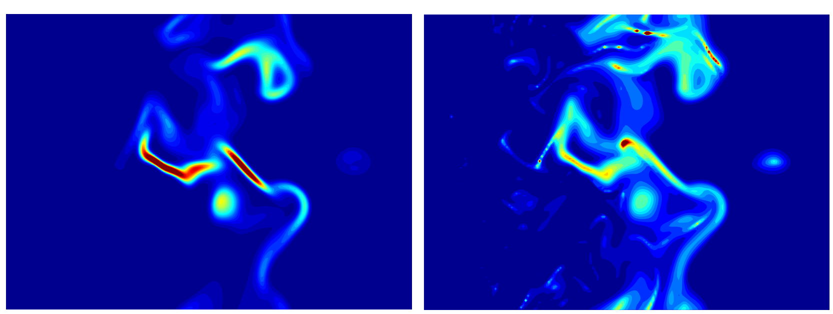

(a) $\dot{\omega}_F/\dot{\omega}_{F,\mathrm{lam}}$ (b) $(\dot{\omega}_F/|\nabla T|)/(\dot{\omega}_{F,\mathrm{lam}}/|\nabla T|_{\mathrm{lam}})$

Fig. 16: Instantaneous 2D slices of a $1.3L \times L$ region centered around the flame showing normalized fuel consumption rate and burning efficiency for case $\mathrm{c}_{n\mathrm{C}7,1}$.

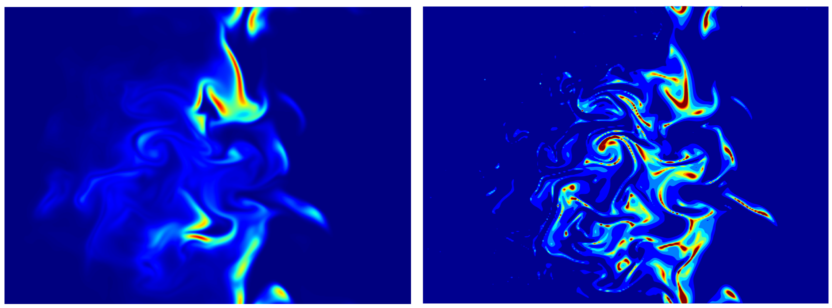

(a) $\dot{\omega}_F/\dot{\omega}_{F,\mathrm{lam}}$ (b) $(\dot{\omega}_F/|\nabla T|)/(\dot{\omega}_{F,\mathrm{lam}}/|\nabla T|_{\mathrm{lam}})$

Fig. 17: Instantaneous 2D slices of a $1.3L \times L$ region centered around the flame showing normalized fuel consumption rate and burning efficiency for case $\mathrm{D}_{n\mathrm{C}7}$.

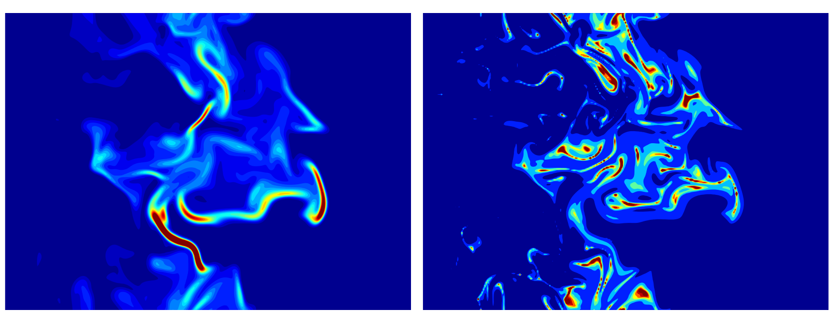

(a) $\dot{\omega}_F/\dot{\omega}_{F,\mathrm{lam}}$ (b) $(\dot{\omega}_F/|\nabla T|)/(\dot{\omega}_{F,\mathrm{lam}}/|\nabla T|_{\mathrm{lam}})$

Fig. 18: Instantaneous 2D slices of a $1.3L \times L$ region centered around the flame showing normalized fuel consumption rate and burning efficiency for case $\mathrm{D}_{n\mathrm{C}7,1}$.